Supplement of Earth Syst. Sci. Data, 18, 1061–1088, 2026
https://doi.org/10.5194/essd-18-1061-2026-supplement

Supplement of

Fusing ERA5-Land and SMAP L4 for an improved global soil moisture product (1950–2025)

Wenhong Wang et al.

Correspondence to: Yonggen Zhang (ygzhang@tju.edu.cn)

Contents of this file

Figures S1- S8 and corresponding descriptions in Sections S1- S4.

Introduction

The supplementary figures include: (1) the spatial distribution and data density of the independent ISMN in situ soil moisture stations used for the historical validation (1960-March 2015) of the adjusted ERA5-Land dataset (Figure S1); (2) a comparison of soil moisture performance over agricultural regions between the adjusted and original ERA5-Land datasets (Figure S2); (3) enlarged regional evaluations of multiple soil moisture products across five continents, including North America, Europe, Asia (mainly China), South America (mainly Brazil), and Africa, based on the normalized Nash-Sutcliffe Efficiency (*NNSE*; Figures S3-S7); and (4) the temporal distribution of ISMN in situ soil moisture observations supporting the historical evaluation and motivating the selection of the 1970-2015 analysis period (Figure S8).

S1. Spatial distribution and data density of ISMN stations used for historical validation

This section presents the spatial distribution and data availability of the independent ISMN in situ soil moisture stations used for the historical validation of the adjusted ERA5-Land dataset. A total of 2,173 stations providing approximately 1.9 million soil moisture measurements over the period January 1960 to March 2015 were collected and retained separately from the primary validation dataset. These observations serve as an independent benchmark to evaluate the reliability of the temporally extended ERA5-Land product. The geographic distribution of these stations and the corresponding data density at each site are shown in Fig. S1.

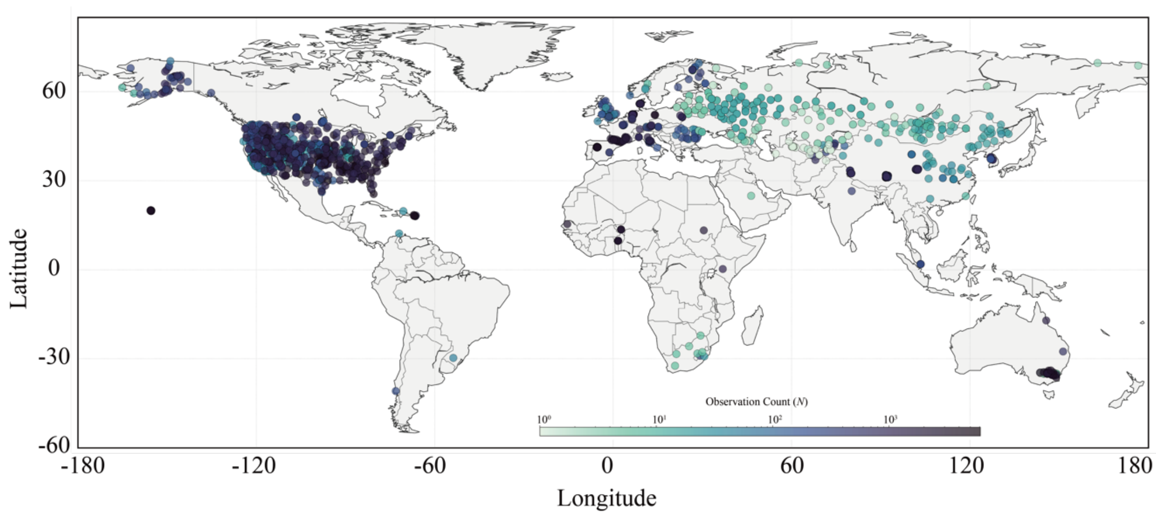

Figure S1. Spatial distribution of the 2,173 independent ISMN in situ stations collected for the historical validation of the adjusted ERA5-Land dataset (1960-March 2015). The color gradient represents the data density available at each station, ranging from sparse records (light green) to dense time series (dark blue).

S2. Comparison between the Adjusted and Original ERA5-Land Datasets over Agricultural Regions

To further assess the product's applicability in human-managed environments, we evaluated the performance of the two datasets at in-situ measurement sites located within agricultural regions. The comparison between the adjusted ERA5-Land and the original ERA5-Land datasets in these regions is shown in Fig. S2.

The results show that the fused product also performs well in agricultural regions, where soil moisture dynamics are more strongly influenced by irrigation, cropping cycles, and other human interventions that are typically underrepresented in reanalysis models such as ERA5-Land. Specifically, the fused dataset reduces the *RMSE* by about 10% and increases the *NNSE* from 0.354 to 0.366 compared with the original ERA5-Land, indicating improved reliability and consistency of soil moisture representation in these human-managed landscapes.

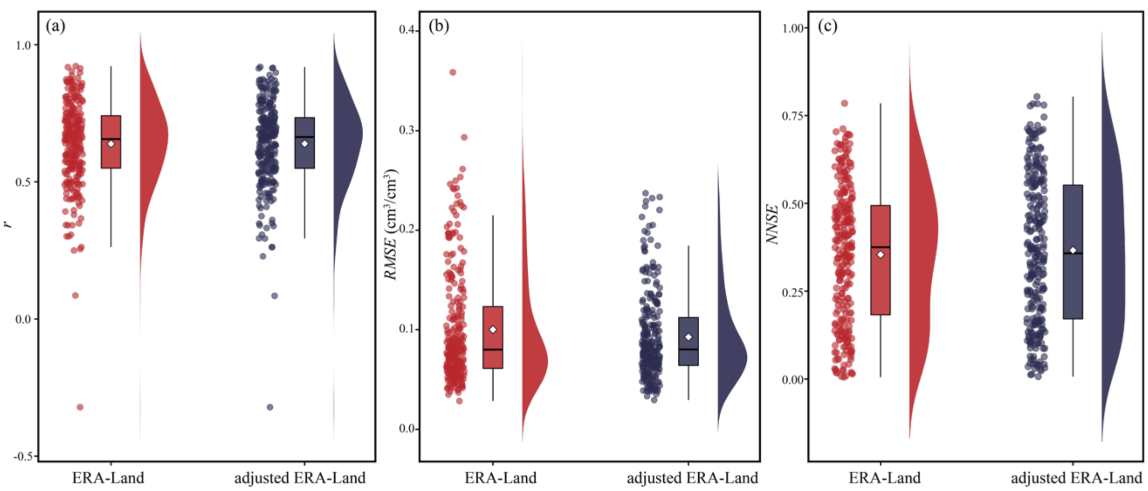

Figure S2. Statistical distributions of performance metrics for the original ERA5-Land (red) and adjusted ERA5-Land (blue) in human-managed agricultural environments. The panels show (a) Pearson correlation coefficient (r), (b) *RMSE*, and (c) *NNSE*. The distributions demonstrate the shift in model performance, boxplots statistics, and probability density curves.

S3. Regional Evaluation across Continents

Figures S3-S7 present the regional evaluation results of four global soil moisture products, including ERA5-Land, ESA CCI, SMAP L4, and the adjusted ERA5-Land, across five continents. Each figure illustrates the spatial distribution of normalized Nash–Sutcliffe efficiency (*NNSE*) values obtained by comparing the soil moisture products with in situ observations.

These supplementary regional maps provide an enlarged and clearer view of the *NNSE* based spatial performance patterns for each product, helping to resolve the regional variations that are difficult to distinguish in the global overview presented in the main text.

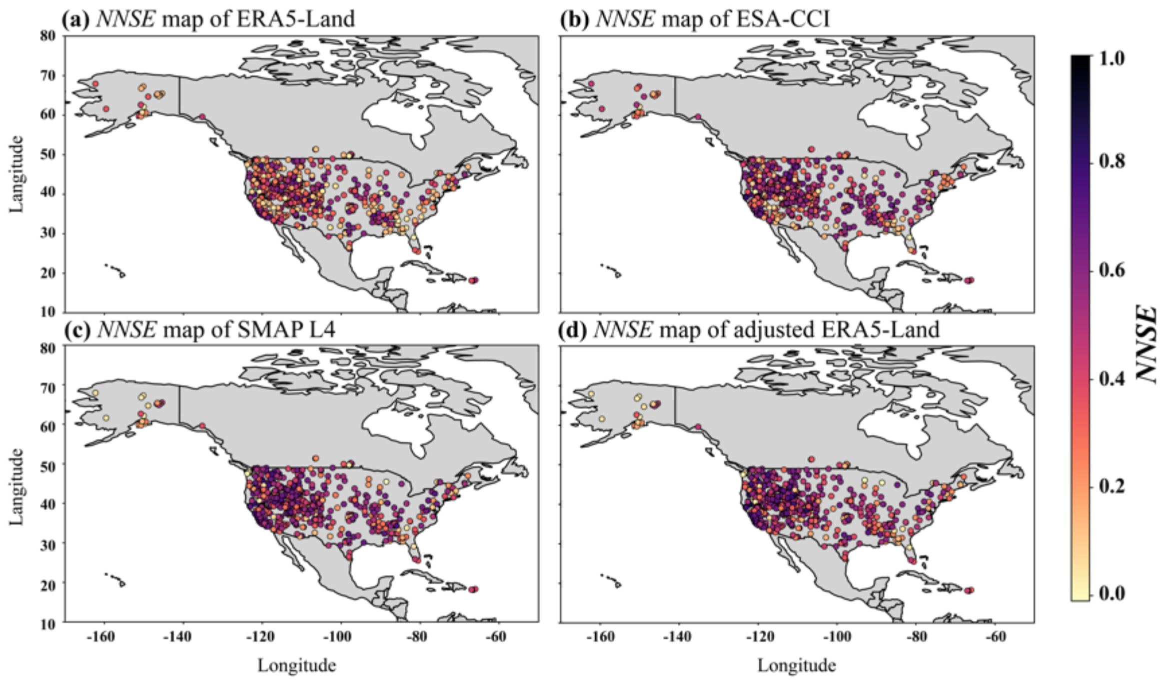

Figure S3. Regional *NNSE* evaluation results for North America. The four panels show *NNSE* values for (a) ERA5-Land, (b) ESA-CCI, (c) SMAP L4, and (d) adjusted ERA5-Land, compared with in situ measurements.

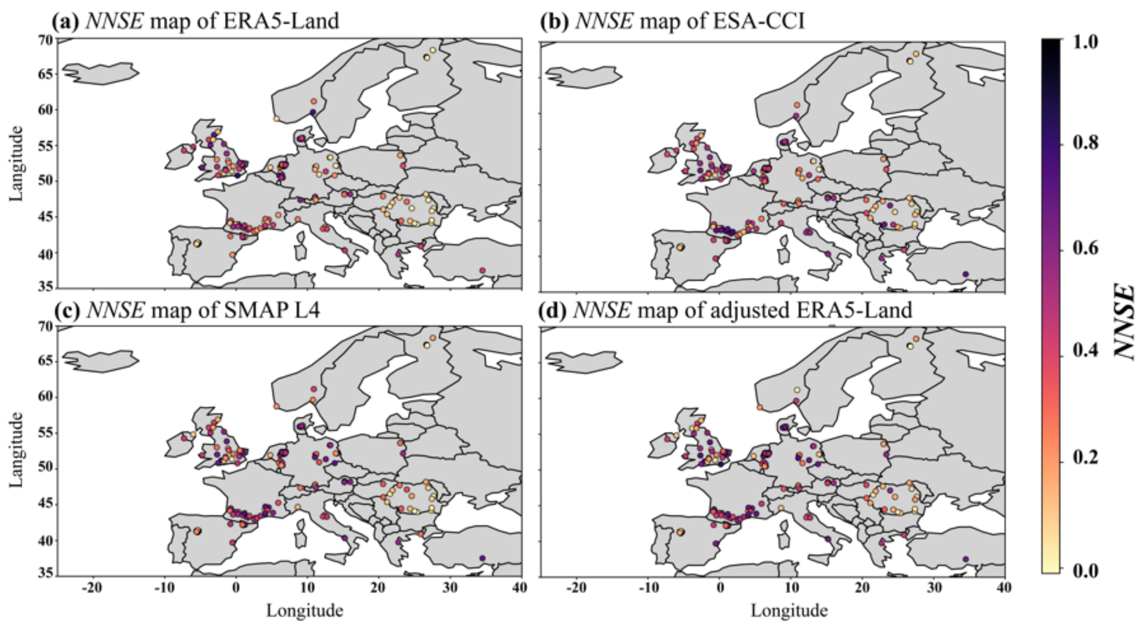

Figure S4. Regional *NNSE* evaluation results for Europe, showing *NNSE* values for (a) ERA5-Land, (b) ESA CCI, (c) SMAP L4, and (d) adjusted ERA5-Land, compared with in situ measurements.

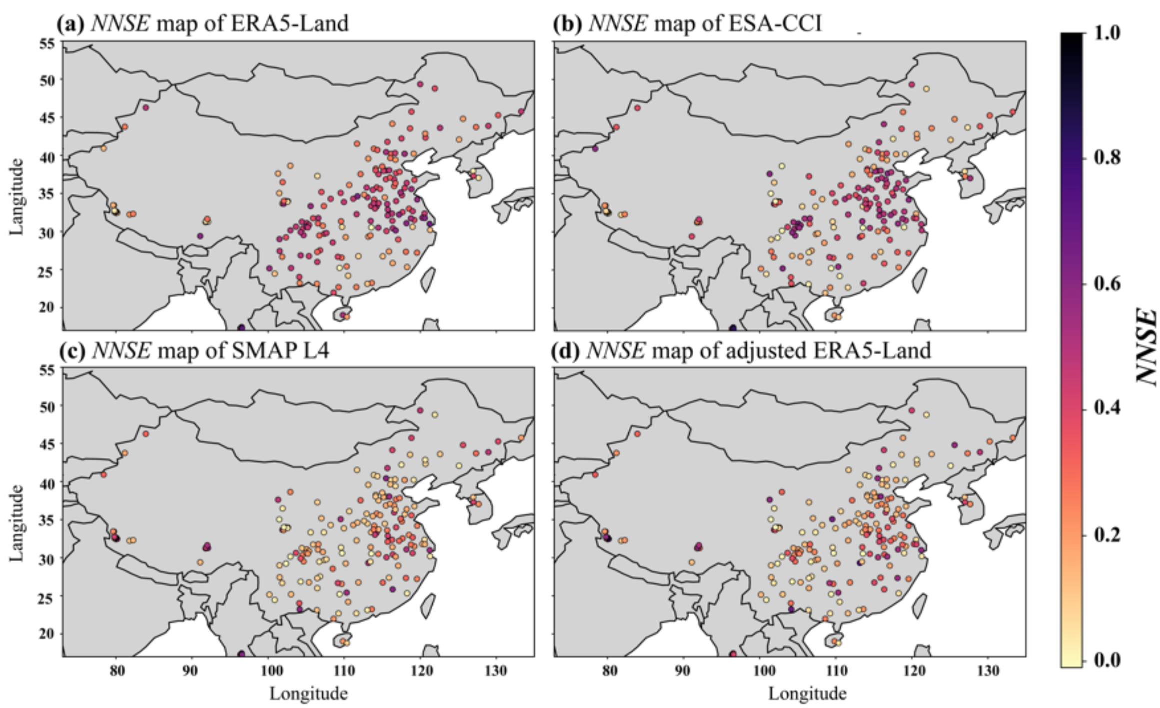

Figure S5. Regional *NNSE* evaluation results for Asia, mainly covering China and surrounding temperate zones.

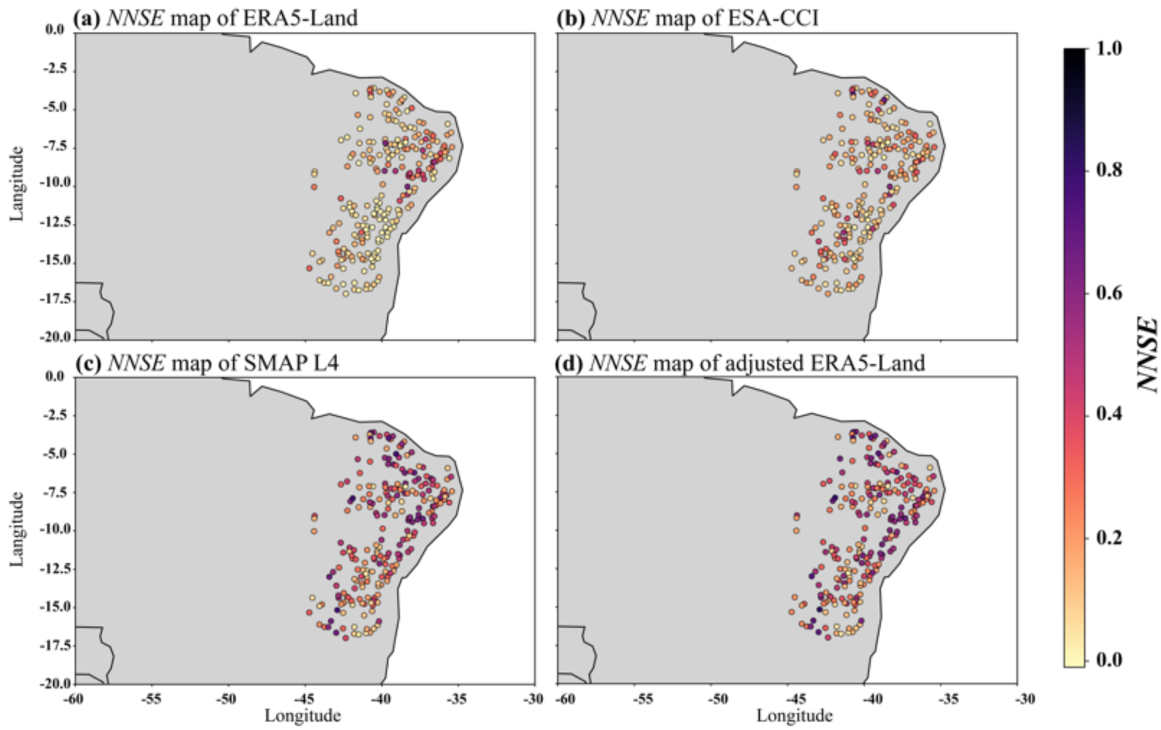

Figure S6. Regional *NNSE* evaluation results for South America, primarily focusing on Brazil.

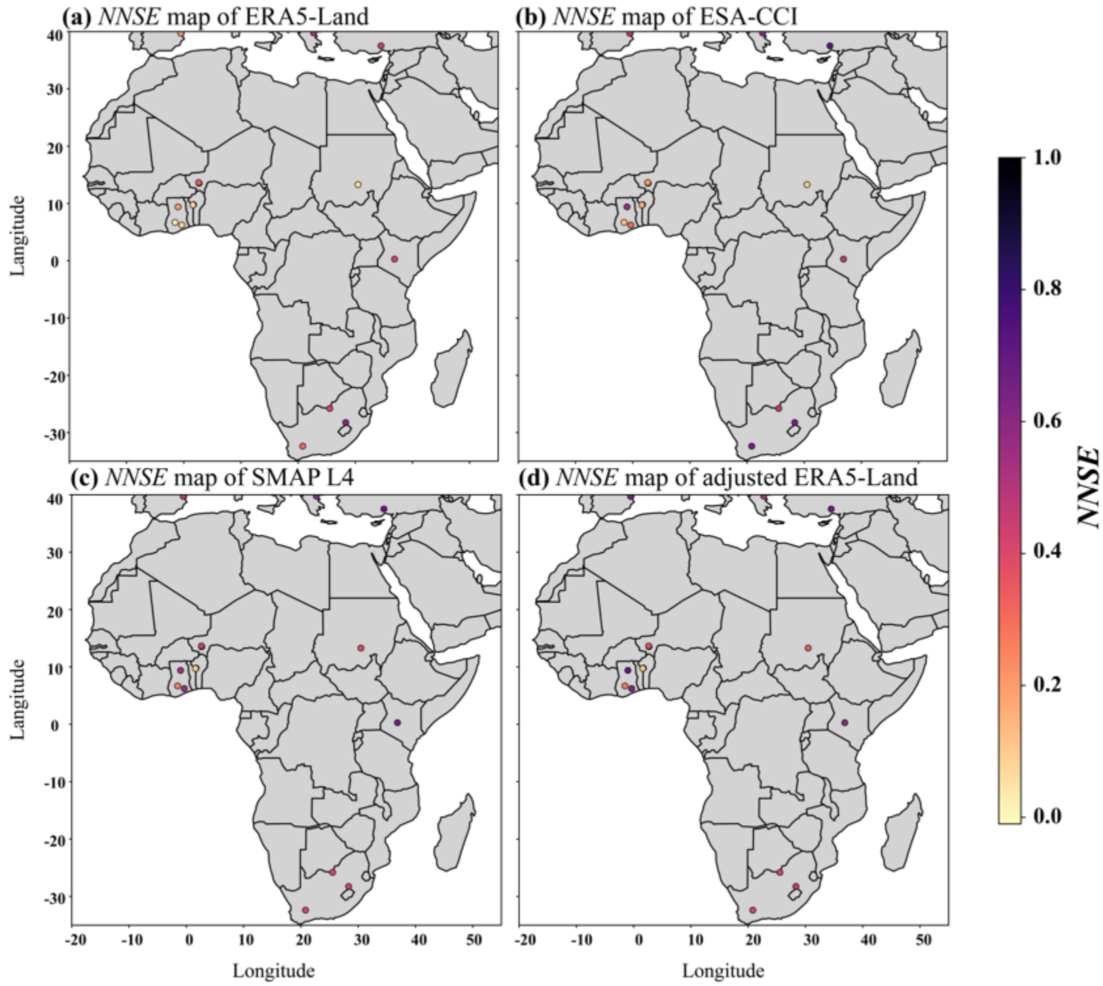

Figure S7. Regional *NNSE* evaluation results for Africa, with limited in situ coverage.

S4. Temporal Distribution of ISMN Observations Supporting the Historical Evaluation

Figure S8 shows the temporal distribution of ISMN in situ soil moisture observations used for the historical validation of the adjusted ERA5-Land dataset over the period 1960-2015. The number of available observations is extremely limited prior to 1970, with fewer than four measurements per year and only 20 observations in total during 1960-1969. It is also evident that the majority of observations are concentrated in the later years, with approximately 99% of the total records occurring after 1998, reflecting the expansion of global in situ soil moisture monitoring networks.

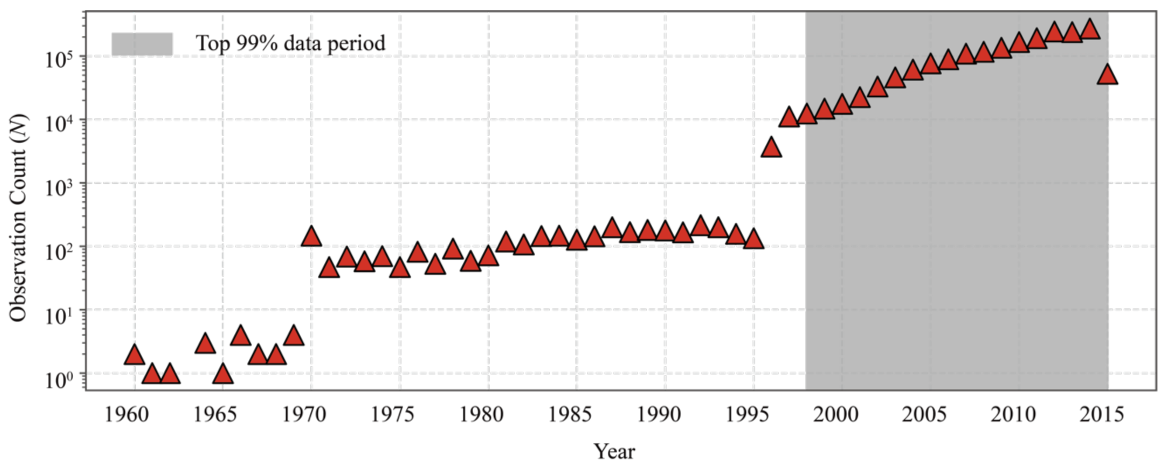

Figure S8. Temporal evolution of the number of available ISMN in situ soil moisture observations used for the historical validation (1960-2015). The period 1960-1970 was excluded from the aggregated statistical analysis in Table 2 due to the extremely sparse data coverage (fewer than 4 observations annually), which prevents robust assessment.